



This is a repository copy of *Straw digestibility in rice: Novel insights from pyrolysis GC-MS and biomass phenotyping*.

White Rose Research Online URL for this paper:

<https://eprints.whiterose.ac.uk/216934/>

Version: Published Version

Article:

Silva, M.P., Whitehead, C., Ordonio, R.L. orcid.org/0009-0005-0212-2508 et al. (7 more authors) (2024) Straw digestibility in rice: Novel insights from pyrolysis GC-MS and biomass phenotyping. *Biomass and Bioenergy*, 182. 107099. ISSN 0961-9534

<https://doi.org/10.1016/j.biombioe.2024.107099>

Reuse

This article is distributed under the terms of the Creative Commons Attribution (CC BY) licence. This licence allows you to distribute, remix, tweak, and build upon the work, even commercially, as long as you credit the authors for the original work. More information and the full terms of the licence here:

<https://creativecommons.org/licenses/>

Takedown

If you consider content in White Rose Research Online to be in breach of UK law, please notify us by emailing eprints@whiterose.ac.uk including the URL of the record and the reason for the withdrawal request.



eprints@whiterose.ac.uk
<https://eprints.whiterose.ac.uk/>



Straw digestibility in rice: Novel insights from pyrolysis GC-MS and biomass phenotyping

Mariana P. Silva^{a,1}, Caragh Whitehead^{a,1}, Reynante L. Ordonio^b, Trinidad C. Fernando^b, Mark Philip B. Castillo^b, Jeremias L. Ordonio^b, Tony Larson^c, Daniel J. Upton^a, Susan E. Hartley^d, Leonardo D. Gomez^{a,*}

^a CNAP, Biology Department, University of York, Wentworth Way, Heslington, York, YO10 5DD, UK

^b Philippine Rice Research Institute, Maligaya, Science City of Muñoz, Nueva Ecija, Philippines

^c Bioscience Technology Facility, Biology Department, University of York, Wentworth Way, Heslington, York, YO10 5DD, UK

^d School of Biosciences, University of Sheffield, Sheffield, UK

ARTICLE INFO

Keywords:

Rice (*Oryza sativa*), straw
Biomass
Saccharification
Pyr-GC/MS
Principal component analysis
p-coumaric acid
Ferulic acid
Silica

ABSTRACT

Valorizing rice straw could mitigate the detrimental health and environmental consequences of disposal through field burning. An essential step for achieving this is reducing straw recalcitrance to digestion by either enzymes or animals to facilitate uses as fertilizer, animal feed, or conversion into fuels and chemicals. In the present work, we developed and characterized a Philippine rice diversity panel to explore the chemical basis of biomass recalcitrance. We used high throughput phenotyping of straw samples from the panel to identify chemical compounds that confer recalcitrance. We determined the saccharification potential, silica, ferulic, and p-coumaric acid content in each rice accession, as well as the chemical fingerprint of biomass composition using pyrolysis followed by GC/MS. Multivariate analysis of the phenotypic data allowed us to characterize the relationship between biomass components and straw saccharification establishing that Si, ferulic acid and coumaric acid are inversely correlated with saccharification. PCA analysis showed that pyrolysis products derived from lignin constitute the largest proportion of compounds inversely correlated with saccharification.

1. Introduction

Large quantities of rice straw are generated globally as rice is one of the main staple foods for human consumption and straw production is unavoidable. It is estimated that as much as 700 million tonnes of rice straw and husk are produced each year globally, and a large amount of this is burned to remove the crop waste from the fields [1–3] with negative impacts on human health and the environment. Straw represents approximately half of the total biomass of the rice plant [4] and is comprised of lignocellulosic material. Conversely, rice straw could represent a large renewable source of biomass with potential for valorization [5]. However, the high silica content and its poor digestibility represent a hurdle for rice straw to be used as feed, fertilizer, or feedstock for biorefineries [6]. Developing uses for rice straw remains a challenge, but given the importance of rice in human nutrition, improving rice straw quality is key to reducing the environmental

impact of this essential staple crop.

One of the main obstacles to valorizing lignocellulosic biomass is its recalcitrance to hydrolysis. Plant cell walls have evolved to resist enzymatic digestion by establishing a network of polymers that are interconnected by covalent and hydrogen bonds, restricting the access of enzymes to their substrates [7]. Crystalline cellulose microfibrils are embedded in an interconnected network of complex matrix polysaccharides and lignin, a phenolic polymer that effectively seals the polysaccharides into a resistant macromolecular structure [8]. The grass cell wall presents substantial differences compared with dicots, particularly in matrix polysaccharides and lignin. In grasses, the major matrix polysaccharides are complex arabinoxylans, highly decorated with hydroxycinnamic acid esters appended to arabinosyl side chains [9]. The ferulic acid (FA) appendages of arabinoxylans can oligomerise with those of neighboring chains or with lignin [10] which, in grasses, contains hydroxycinnamic acid units in its structure [11]. These crosslinks

* Correspondence author.

E-mail address: leonardo.gomez@york.ac.uk (L.D. Gomez).

¹ Both authors contributed equally to the paper.

help to increase the resistance of the biomass to enzymatic attack. Reducing lignocellulose recalcitrance could facilitate alternative uses of rice straw, generating extra income for farmers. Changes in cell wall components in rice can affect straw recalcitrance, as shown by several studies to improve energy crops and processing alternatives [12,13]. The efforts to reduce recalcitrance in grasses have been directed at reducing lignin content [14] and reducing ester bonds between hydroxycinnamic acids and hemicellulose and lignin [15]. The availability of gene editing approaches that allow precise targeting of saccharification bottlenecks [16].

Rice is the highest Si accumulator in *Graminae*, and among the multiple beneficial effects that Si has in plants, it is regarded as a defense against herbivores due to the physical strengthening of the cell wall [17]. As a cell wall component, it interacts with cell wall polymers and co-regulates the composition and processing characteristics of rice straw [18]. Reducing the content of Si in rice cultivars by increasing N supply, increases saccharification of the resulting biomass [19]. Indeed, removal of the Si content using alkaline pretreated increases enzymatic hydrolysis of rice husks several folds [20].

Phenotyping large populations to assess differences in cell wall composition and digestibility requires high-throughput approaches that can cope with the large populations necessary to capture genetic diversity. Whilst such high-throughput approaches are now available for measurement of silica [21], the intrinsic chemical complexity of plant cell walls presents an analytical challenge. Spectroscopic approaches such as Fourier transformed infrared spectroscopy and near infrared spectroscopy (NIRS) have been applied to study plant populations and establish cell wall characteristics associated with saccharification [22, 23]. In rice, NIRS has been applied to identify lignocellulose recalcitrant factors in transformed lines and recombinant inbred lines [24,25]. These approaches, however, require the development of wet chemistry based models in order to gain precision.

Advances in mass spectrometry-based metabolomics and data processing techniques allow for large-scale analysis of untargeted metabolic profiles [26]. Analytical pyrolysis coupled with gas chromatography/mass spectrometry (Pyr-GC/MS) has been successfully used for the characterization of complex natural polymers, such as lignin and polysaccharides [27–29]. The resulting pyrograms represent the fingerprint pattern of the samples, allowing a synthetic visualization of high-dimensional data and the relationships between different variables [27–29].

In the present study, we characterised the straw from field-grown rice varieties from the Philippines using analytical (Pyr-GC/MS) combined with phenotyping for saccharification potential, silica determination and hydroxycinnamic acid content. We explored the suitability of Pyr-GC/MS and PCA as a fingerprinting technique to identify the basis of straw recalcitrance.

2. Materials and Methods

2.1. Rice population and plant materials

The PhilRice association panel comprised 215 rice genotypes from the Philippines, which originate from two *Oryza sativa* subspecies: *indica* and *nerica*. These genotypes were selected from a number of different sources (76 released and 14 traditional varieties plus 125 elite lines). These genotypes are expected to be highly inbred lines with a homozygous genomic background. (See the Supplemental file Fig. S1 and Table S2 for the list of the population used).

The association panel was grown in the field (N 15° 40'09"N 120° 53'45"E, 2017DS & 2018DS) at the Philippines Rice Research Institute, Science City of Muñoz, Philippines. The field trial was conducted in randomized plots of 10 m² at a plant density of 40 plants/m². Each straw sample was collected from the main tiller of five plants after harvesting for grain, and 5 replicates were grown for each genotype. The straw collected was dried for two days in the open air. Straw samples were

kept in separate paper bags and sent to the Centre for Novel Agricultural Products (CNAP), University of York, UK for characterisation. The rice stems (minus nodes) were cut into small pieces, then ground to a fine powder using a cyclone mill (Retsch UK, 1 mm sieve) and stored. These samples were used for assays including saccharification, Pyr-GCMS and total lignin content.

2.2. Ferulic (FA) and p-coumaric acid (CA) determination

Alkaline extraction of CA and FA was performed according to Fry 2000 [30]. Approximately 10 mg of dry plant material was ball milled and 1 ml of 1 M NaOH was added and the samples were incubated shaking at 140 rpm at 30 °C overnight. The reaction was neutralized by addition of 100 µl 99% TFA and phase extracted twice using butanol. The butanol was evaporated, and the pellet resuspended in 200 µl MeOH. Samples were analyzed by LC/MS. Separation was carried out on an Acquity I class LC system (Waters UK, Elstree) using a BEH C18-1.7µ 2.1 × 100mm (Waters), the mobile phases were A) 0.1% acetic acid in H₂O, and B) 0.1% acetic acid in acetonitrile. The gradient started at 20% B, and increased to 100% B over 3.25 min, where it remained for 0.15 min. The gradient returned to 20% B over 0.05 min, and re-equilibrated over 0.55 min. The total duration of the program was 4 min. The flow rate was 0.5 ml min⁻¹, and the injection volume 3 µl. The detector used was a TSQ EnduraTM triple quadrupole mass spectrometer (Thermo Fisher Scientific, Altrincham, UK) with a HESI source, operated in negative MRM mode. Commercially purchased standards of CA and FA (Sigma) were used to construct standard curves in the range from 12 to 400 µM.

2.3. Saccharification determination

Saccharification potential was determined using an automated robotic platform as previously described [31]. In brief, loading of plant powder into 96-well plates was done using a custom-made robotic platform (Labman Automation, Stokesley, North Yorkshire, UK), and saccharification assays were performed after water pretreatment at 94 °C for 30 min. Enzymatic hydrolysis was carried out using an enzyme cocktail with a 4:1 ratio of Celluclast and Novozyme 188 (Novozymes Enzymes).

2.4. Analytical pyrolysis-gas chromatography-mass spectrometry (Pyr-GC/MS)

Individual powdered rice straw samples were subject to Pyr-GC/MS analysis. Pyr-GC/MS results were obtained using a CDS 5250-T Trapping Pyrolysis Autosampler, Agilent Technologies 7890B GC System as gas chromatography unit and Agilent Technologies 5977A MSD as mass spectrum unit. The samples were pyrolyzed at 450 °C for 15 s, under trapping mode. The volatile materials released were carried into the GC/MS unit, via a heated transfer line (340 °C) in a helium flow for GC/MS analysis. The following GC/MS parameters were applied: GC inlet temperature at 350 °C, the initial temperature at 40 °C for 2 min, ramp rate at 10 °C/min until 300 °C, holding at 300 °C for 12 min, split ratio 50:1. Helium carrier gas flow was 1 ml/min and the separation was performed using an Agilent HP-5ms Ultra Inert (30 m × 0.25 mm × 0.25 µm) column. Volatile compounds were identified by comparing the mass spectra with NIST 14 library database (Match ≥85%).

Three spectra for each sample were collected, and the triplicate-averaged spectrum was used for principal component analysis (PCA). PCA was carried out using The Unscrambler X 10.5.1 software (CAMO). Peak identification was initially done manually using MassHunter Qualitative Analysis B.07.00 and NIST 14 library.

Before PCA analysis, the acquired data were processed according to the methodology previously described [32–36]. This process produced a matrix of baseline corrected peak areas for samples × unique mass tags (*m/z* and retention time), for further analysis.

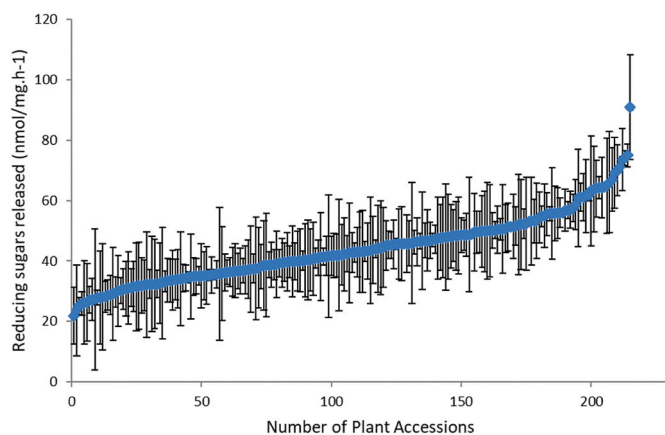


Fig. 1. Range of saccharification values obtained for the rice association panels.

2.5. Determination of silicon and lignin

Silicon (Si) in pellets of ground straw was determined using a portable X-ray fluorescence spectrometer and ground biomass pellets following the method validated by Reidinger et al. [21]. Lignin content was quantified using acetyl bromide [37]. Three replicates (4 mg) from each straw sample were used for lignin determination following the procedure previously described [38]. Lignin content ($\mu\text{g}\cdot\text{mg}^{-1}$ cell wall) was determined using the following formula: $(\text{Absorbance} \div (\text{coefficient} \times \text{path length})) \times ((\text{total volume} \times 100\%) \div \text{biomass weight})$. The coefficient for grasses (17.75) was used for rice.

3. Results

3.1. Saccharification

Lignocellulose recalcitrance to digestion was measured by incubating ground straw from 215 individual genotypes with a commercial cellulase cocktail following a water pre-treatment at 94 °C using an automated platform as reported by Gomez et al. [31]. The straw was harvested in the spring season of 2017 and the material used for saccharification was carefully selected to include stem tissue of

equivalent age. The saccharification results show values between 21.48 and 90.84 nmol of reducing sugar equivalents/mg of biomass per hour of hydrolysis (nmol/mg.h) (Fig. 1). These values present a 4.2-fold variation in saccharification potential, indicating that saccharification represents a trait with a wide range of phenotypic variation in our association panel. In a recent study, Nguyen et al. used the same platform to determine the saccharification potential in a rice association panel from Vietnam [38]. The Vietnamese association panel presented values ranging between 20 and 134 nmol/mg.h in two consecutive years (2013 and 2014) under field conditions, therefore showing a phenotypic variation similar to the PhilRice association panel.

3.2. Pyr-GC/MS analysis of rice straw

The PhilRice association panel was characterized by Pyr-GC/MS fingerprinting of each of the rice varieties in the panel to identify pyrolysis peaks that associate with the recalcitrance of rice straw to enzyme digestion.

The composition of the straw in the PhilRice population was typically 30% cellulose, 20% matrix polysaccharides, and the lignin content varied between 13.72 and 20.87%, while Si had an average content of 7% (Supplementary Table S1). FA and CA content ranged between 0.78 and 3.99 mg/g and 2.85–8.95 mg/g respectively (Supplementary Table S2). The role of feedstock composition in determining pyrolysis yields has been shown in numerous studies [39]. The differences in composition of the straw material in our rice panel (cellulose, hemicellulose, lignin, FA and CA) will determine the pyrolytic behavior of the materials.

Seventy compounds, comprising 92% of the total area in the pyrogram, could be compared through GC-MS analyses among the 167 peaks detected initially (Supplementary Table S3 and Table S4). A total of 37 compounds, representing 55.88% of the total area in the pyrogram, were identified through GC-MS analyses, using the NIST Lab database with a Match $\geq 85\%$ from the 70 peaks. Among them, twenty compounds (26.27% of the total area) were categorized as aromatic hydrocarbons, furans, hydrocarbon derivatives, oxygenated, and nitrogen-containing substances (NIST Lab database with a Match $\leq 85\%$), based on their fragmentation pattern. Thirteen compounds (constituting 9.91% of the total area) remained unidentified within the 70 peaks compared. Fig. 2 illustrates a typical chromatogram for rice straw samples analyzed using the pyrolysis conditions described in the Methods section.

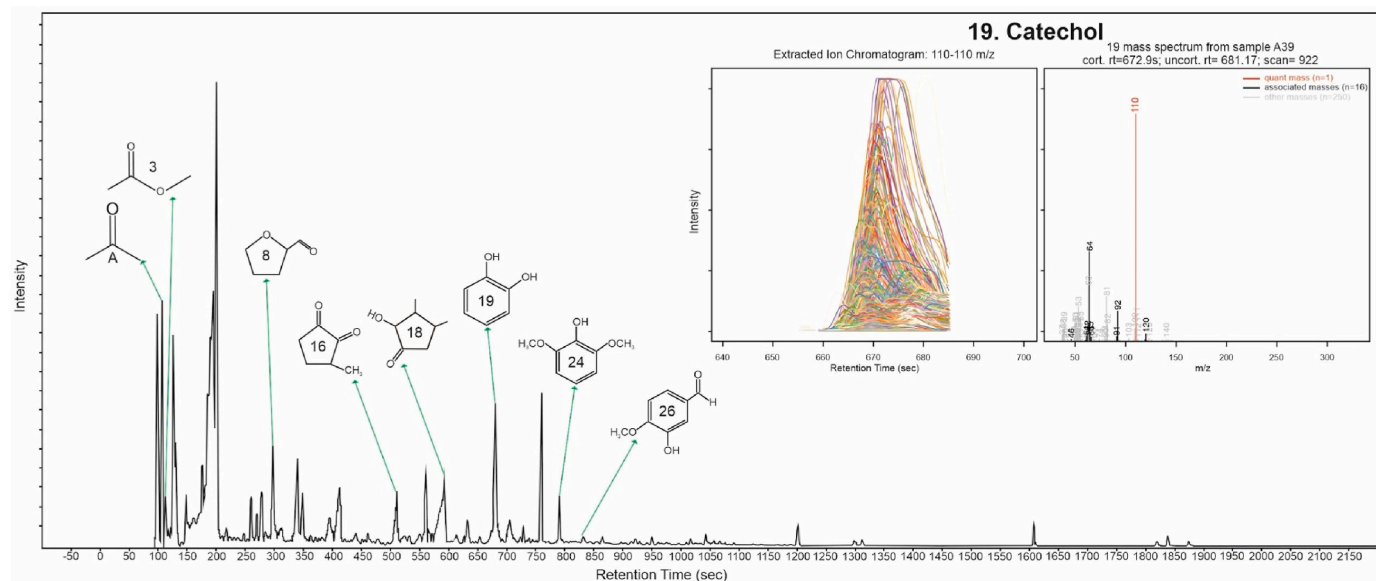


Fig. 2. Chromatogram of pyrolyzed rice straw. A: acetone, 3: acetic acid, methyl ester, 8: furfural, 16: 3-methylcyclopentane-1,2-dione, 18: 2-cyclopenten-1-one, 2-hydroxy-3,4-dimethyl, 19: catechol, 24: 2,6-dimethoxy, phenol, 26: 3-hydroxy-4-methoxy-benzaldehyde.

Table 1

Peak list from Pyr-GC/MS from the PhilRice population samples. Retention time (RT), ID numbers, compound names (NIST 14 library database -Match $\geq 85\%$ -), peaks are derived from Carbohydrate (C), Lignin (L) and Other (O) and m/z of detected fragments.

RT (seconds)	ID	Name	From	m/z
102	M44T102	Acetaldehyde	C	44 43 42 41 45 40 49 51 37
103	M47T103	Unknown	U	47 48 46
110	M56T110-M68T110	acetone	C	58 43 42 39 41 38 56 44 37
112	M59T112	acetic acid, methyl ester	C	74 43 42 59 44 41 45 75
113	M58T113	2-propen-1-ol	C	57 58 55
150	M150T750+M150T760	2-methoxy-4-vinylphenol	L	150 77 135 107 79 51 78 53 63 39
159	M45T159	3-hydroxy-2-butanone	C	45 43 88 42 44 46 41
159	M60T159	acetic acid	C	45 60 44
176	M60T176	Unknown	U	60 45 43 42 41 44 61 40 46
177	M45T177	oxygenated compounds	O	43 45 42 41 39 69 73 81 80 59
189	M75T189	Unknown	U	74 38 57 37 53 55 40 56 58
189	M74T189+ M74T173	organic nitrogen-containing compounds	O	74 42 45 43 44 41 39 38 37 75
197	M90T197	acetic acid, hydroxy-, methyl ester	C	59 61 42 90 60 62 44 75 40 68
234	M91T234	Unknown	U	86 91 58 92 44 63 62 87 93 52
241	M89T241	Unknown	U	88 56 41 39 58 55 53 38 37 59
246	M88T246	Unknown	U	88 56 41 39 58 55

Table 1 (continued)

RT (seconds)	ID	Name	From	m/z
265	M102T265	Unknown	U	53 38 37 59 102 42 44 41 39 59 38 55 37 103
275	M96T275	3-furaldehyde	C	95 96 39 41 38 67 37 86 80 40
300	M96T300	furfural	C	96 82 95 39 38 53 54 41 37 98
309	M96T309	oxygenated compounds	C	43 39 96 95 82 54 38 41 42 53
328	M96T328	oxygenated compounds	C	98 55 39 69 41 53 42 70 96 57
334	M98T334	2-furanmethanol	C	94 66 65 39 40 55 63 38 95 50
341	M116T341	1- acetyloxy, 2-propanone	C	86 42 116 73 44 96 57 68 74 40
349	M95T349	Furans	C	43 95 110 38 55 51 50 37 52 96
360	M98T360	Unknown	U	98 68 83 112 57 58 45
363	M95T363	1-(2-furanyl)- ethanone	C	95 110 39 43 38 37 50 111
373	M98T373	Furans	C	41 98 53 67 51 50 95 52 81 109
403	M98T403	1,2 cyclopentanedione	C	98 55 42 69 43 41 39 70 99 40
431	M106T431	aromatic hydrocarbons	L	110 39 105 77 106 42 51 40 54 82

(continued on next page)

Table 1 (continued)

RT (seconds)	ID	Name	From	m/z
436	M130T436	Unknown	U	110 109 57 43 53 67 39 81 51
450	M101T450	2,4-dihydroxy-2,5-dimethyl-3(2H)-furanone	C	43 55 39 101 41 73 144 45 98 69
459	M94T459	Phenol	L	94 66 65 39 55 63 38 95 50
465	M140T465	2-furanmethanol, acetate	L	81 98 53 140 52 56 43 80 97 122
475	M114T475	organic nitrogen-containing compounds	O	114 58 57 42 85 115 98 59 86
505	M112T505	3-methylcyclopentane-1,2-dione	C	112 55 69 57 41 83 56 84 43 39
535	M109T535	oxygenated compound	C	126 43 95 39 69 111 41 55 83 56
553	M128T553	Furans	C	43 128 57 45 58 44 72 129
553	M158T553	Furans	C	43 57 128 124 69 54 45 53 123 67
573	M43T573	2-Cyclopenten-1-one, 3-ethyl-2-hydroxy-	C	43 44 39 57 55 41 42 126 53 83
579	M44T579	Pentanal	C	44 57 43 39 41 42 55 45 53 40
591	M126T591	2-cyclopenten-1-one, 2-hydroxy-3,4-dimethyl	C	126 69 111 43 55 41 83 56 39 97

Table 1 (continued)

RT (seconds)	ID	Name	From	m/z
617	M134T617	1-ethenyl-4-methoxybenzene.	L	134 91 119 65 63 135 89 92 62 103
621	M102T621	Unknown	U	102 56 57 45 42 103 58 61 46 38
654	M110T654	aromatic hydrocarbons	L	138 123 95 67 77 53 51 65 43 66
666	M142T666	oxygenated compound	O	142 68 85 71 113 67 140 53 40 69
672	M110T672	Catechol	L	110 64 81 53 111 82 54 79 68
675	M85T675	oxygenated compound	C	85 43 57 86 42 56 44 58
679	M120T679	2,3-dihydro-benzofuran,	L/C	120 91 65 39 63 119 62 51 50 94
702	M97T702	Unknown	U	97 125 51 43 128 44 79 85 91 56
730	M137T730	aromatic hydrocarbons	L	137 166 81 109 51 53 77 135 138 91
734	M132T734	2,3-dihydro, 1H-inden-1-one	O	104 132 78 103 51 77 131 67 50 76 180
737	M100T737	Furans	C	43 100 55 99 39 85 124

(continued on next page)

Table 1 (continued)

RT (seconds)	ID	Name	From	m/z
				41 42
				73
771	M182T771	Unknown	U	108
				39 43
				126
				136
				111
				52 53
				78 41
791	M154T791	2,6-dimethoxy, phenol	L	154
				139
				96
				111
				93 65
				39 68
				51 53
797	M151T797	Unknown	U	57 41
				109
				69 81
				59 68
				151
				87
				135
811	M151T811	Unknown	U	39
				151
				150
				94 66
				67 78
				74
				146
				149
814	M127T814	oxygenated compound	O	57 55
				127
				99 39
				100
				41 53
				101
				42
820	M130T820	Unknown	U	123
				130
				152
				124
				131
				109
				68 81
				67
				153
833	M151T833	3-hydroxy-4-methoxy- Benzaldehyde	L	151
				166
				123
				150
				178
				107
				77
				108
				79 52
865	M168T865	hydrocarbons derivative	L	168
				125
				153
				53 41
				107
				110
				169
				82
				118
866	M164T866	2-Methoxy-4-(1- propenyl)-phenol	L	164
				149
				91 77
				103
				131
				121
				55
				133
				104

Table 1 (continued)

RT (seconds)	ID	Name	From	m/z
922	M167T922	aromatic hydrocarbons	L	167
				182
				79 77
				107
				168
				53
				123
				65
				121
927	M180T927	1-(4-hydroxy-3- methoxyphenyl)-2- propanone	L	137
				180
				122
				43 94
				138
				66 51
				77 65
951	M180T951	3',5'- dimethoxyacetophenone	L	180
				165
				137
				77
				122
				91 65
				181
				94 51
972	M170T792	Unknown	U	138
				57 94
				66
				147
				148
				8127
				89 90
1014	M190T1014	hydrocarbons derivative	L	147
				176
				148
				45 41
				181
				73 81
				92
				177
1044	M194T1044	(E)-2,6-dimethoxy-4- (prop-1-en-1-yl)phenol	L	194
				91
				119
				179
				77
				131
				79
				103
1140	M242T1140	pentadecanoic acid	O	73 60
				43 41
				55 57
				129
				71 69
				199
1203	M256T1203	n-hexadecanoic acid	O	73 60
				43 55
				57 41
				129
				69 71
				256
1301	M67T1301	octadecanoic acid isomer	O	67 81
				95 82
				68 96
				79 54
				109
				110
1304	M264T1304	octadecanoic acid isomer	O	55 69
				41 83
				97 43
				57 84
				70 56
1313	M43T1313	octadecanoic acid	O	73 43
				60 57
				55 41

(continued on next page)

Table 1 (continued)

RT (seconds)	ID	Name	From	m/z
				129
				69 71

The 70 compounds selected were classified into three distinct classes based on the fraction from which they originated: Carbohydrate (C), Lignin (L), Others (O), and unknown (U) (Table 1). C and L compounds were the most abundant in all samples, contributing 38.03% and 25.35% of the total peaks respectively. O compounds were ca. 15.49% and U 22.53% (Table 1 and Supplemental Table S1).

The lack of information on the pyrolytic behavior of all the components of the network of polymers in the 215 rice straw accessions precludes the identification of 44.12% of the compounds. However, the metabolite fingerprinting approach that we selected does not require a complete metabolite identification to assess the quality of rice straw related to saccharification [32,40]. A principal component analysis (PCA) was applied to the 167 distinct peaks to visualize and characterize the differences or similarities between samples.

3.2.1. Principal component analysis of saccharification and pyrolysis

Separate PCA were conducted for the pyrolysis peaks of the 215 rice accessions (Fig. 3A), or in combination with saccharification potential data (Fig. 3C). In these PCA scores plots, each point represents the data obtained for one accession. When the pyrolysis data is analyzed alone, the scores plot shows that 68% of the total variation is explained by the first two principal components (PCs), with PC1 describing 44% of the

validated variance and PC2 describing 24% (Fig. 3A). When we added the saccharification data into the analysis, the scores plot shows that an overall 87% of the total variation is explained by the two first components, where PC1 explains 76% of the validated variance and PC2 explains 11% (Fig. 3C). There are no distinct clusters of accessions in the score plot without added saccharification data (Fig. 3A) indicating that the overall pyrolysis data does not define any sub-groupings for straw composition. However, when saccharification was included in the analysis, the score plot shows that the samples are not randomly distributed (Fig. 3C). In Fig. 3D, the angle between saccharification and PC1 is close to zero, therefore PC1 completely describes saccharification. Moving from left to right (PC1) along the score plot in Fig. 3C—a pattern can be observed; indicating that samples with the same color and shape have similar average values for saccharification. Using the loading plots in Fig. 3B and D, we selected between 41–36 peaks with loadings ranging from $-1/-0.5$ or $1/-0.5$ (Table 1). Out of the 41 peaks selected, we identified a subset of 36 compounds based in their mass spectra using the NIST Lab database (Match $\geq 85\%$) (Table 2). The fingerprints of loading plots Fig. 3B and D were determined by 41 and 36 compounds, respectively (Table 2), with important differences in the percentage in which each class of compounds was represented. The loading plot in Fig. 3B is characterised by a similar contribution of C (34.15%) and L (34.15%) compounds, followed by O (14.63%) and U (17.07%) compounds. In contrast, the loading plot in Fig. 3D is characterised by a major contribution of L (34.14%) followed by C (24.39%), and a similar contribution of O (12.20 %) and U (12.20%).

The main compounds identified in the C group were, 3-methyl-1,2-cyclopentanedione (16), 2-hydroxy-3,4-dimethyl-2-cyclopenten-1-one (18), furans (23), 1-acetyloxy 2-propanone (10), 1,2

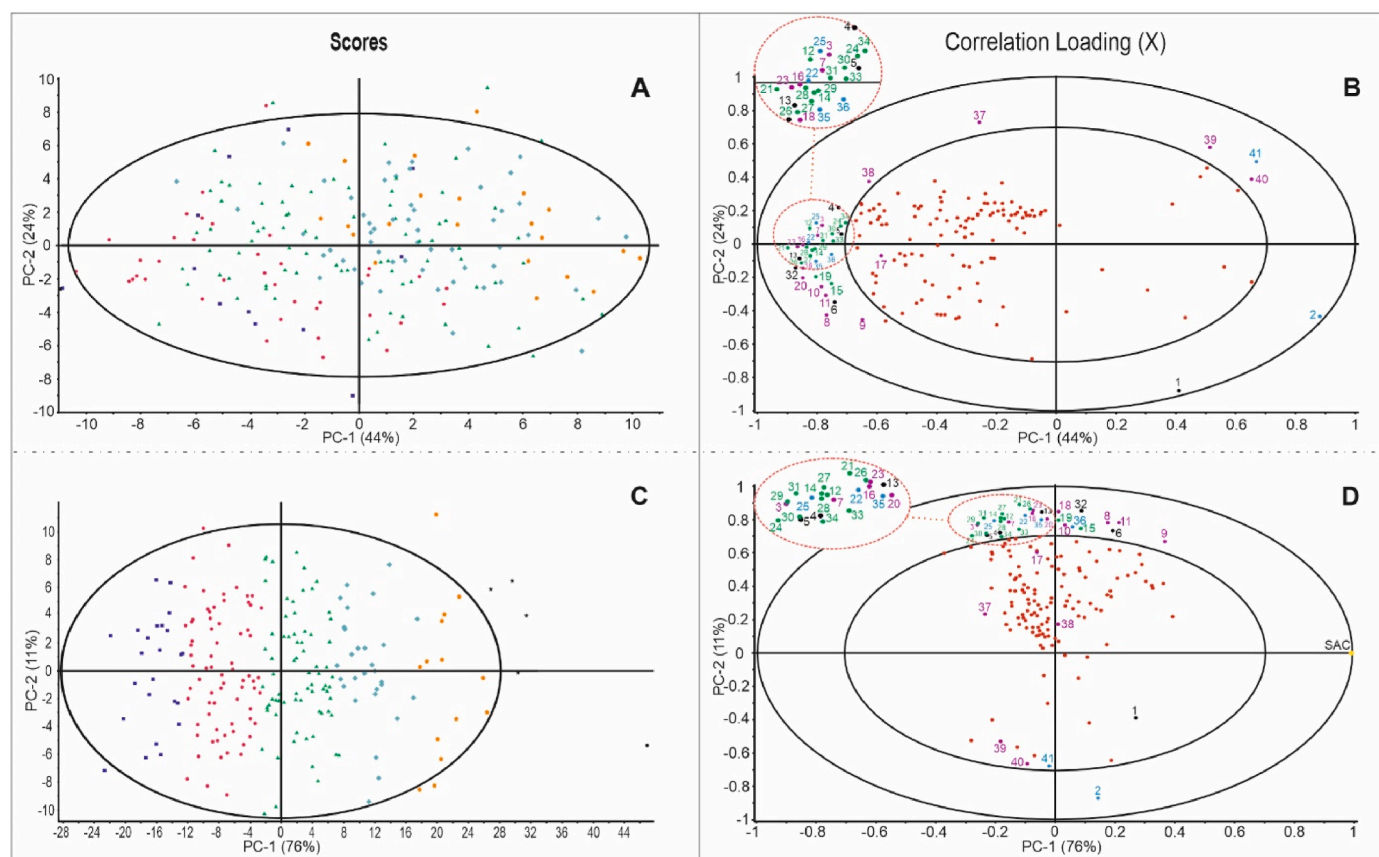


Fig. 3. Principal component analysis of pyrolysis derived compounds and saccharification in the PhilRice population. A–C: Score plots, the clusters of accessions are represented by dots of the same color and shape. B–D: Loading plots, peaks are labelled in different colours according to their origins: derived from Carbohydrate (purple), Lignin (green), Other (blue), and Unknown (black). Unselected peaks (red) and saccharification (yellow). The areas inside the red ellipses are amplified to facilitate the identification of the samples. (For interpretation of the references to color in this figure legend, the reader is referred to the Web version of this article.)

Table 2

Peak list of subsets of 41 compounds from PCA of pyrolysis derived compounds and saccharification. Number PCA (NP), Retention time (RT), ID numbers, compound names (NIST 14 library database -Match $\geq 85\%$), peaks are derived from Carbohydrate (C), Lignin (L) and Other (O).

NP	RT (secs)	ID	Name	From
1	176	M60T176	Unknown	U
2	177	M45T177	oxygenated compounds	O
3	197	M90T197	acetic acid, methyl ester	C
4	234	M91T234	Unknown	U
5	246	M88T246	Unknown	U
6	265	M102T265	Unknown	U
7	275	M96T275	3-furaldehyde	C
8	300	M96T300	furfural	C
9	334	M98T334	2-furanmethanol	C
10	341	M116T341	1-acetyloxy, 2-propanone	C
11	403	M98T403	1,2 cyclopentanedione	C
12	431	M106T431	aromatic hydrocarbons	L
13	436	M130T436	Unknown	U
14	459	M94T459	Phenol	L
15	465	M140T465	2-furanmethanol, acetate	L
16	505	M112T505	3-methylcyclopentane-1,2-dione	C
17	535	M109T535	oxygenated compound	C
18	591	M126T591	2-cyclopenten-1-one, 2-hydroxy-3,4-dimethyl	C
19	672	M110T672	Catechol	L
20	675	M85T675	oxygenated compound	C
21	730	M137T730	aromatic hydrocarbons	L
22	734	M132T734	2,3-dihydro, 1H-inden-1-one	O
23	737	M100T737	Furans	C
24	791	M154T791	2,6-dimethoxy, phenol	L
25	814	M127T814	oxygenated compound	O
26	833	M151T833	3-hydroxy-4-methoxy-Benzaldehyde	L
27	865	M168T865	hydrocarbons derivative	L
28	866	M164T866	2-Methoxy-4-(1-propenyl)-phenol	L
29	922	M167T922	aromatic hydrocarbons	L
30	927	M180T927	1-(4-hydroxy-3-methoxyphenyl)-2-propanone	L
31	951	M180T951	3',5'-dimethoxyacetophenone	L
32	792	M170T792	Unknown	U
33	1014	M190T1014	hydrocarbons derivative	L
34	1044	M194T1044	(E)-2,6-dimethoxy-4-(prop-1-en-1-yl) phenol	L
35	1140	M242T1140	pentadecanoic acid	O
36	1203	M256T1203	n-hexadecanoic acid	O
37	573	M43T573	2-Cyclopenten-1-one, 3-ethyl-2-hydroxy-	C
38	579	M44T579	Pentanal	C
39	102	M44T102	acetaldehyde	C
40	113	M58T113	2-propen-1-ol	C
41	189–173	M74T189+ M74T173	organic nitrogen-containing compounds	O

cyclopentanedione (11), 2-furanmethanol (9), acetic acid methyl ester (3), and furfural (8). Lignin derived compounds were represented by syringol and guaiacol derivatives such as, catechol (19), 3-hydroxy-4-methoxy-benzaldehyde (26), phenol (14), and 2,6-dimethoxyphenol (24).

Similar relationships between pyrolysis products were found in the PCA loading plots in Fig. 3B and D. Compounds such as 3-methylcyclopentane-1,2-dione (16), 2-cyclopenten-1-one, 2-hydroxy-3,4-dimethyl (18) and furfural (8), included in the C group, show a positive correlation between themselves and with the L derived compounds Catechol (19), 3-hydroxy-4-methoxy-benzaldehyde (26) and 2,6-dimethoxyphenol (24). All these compounds present a negative correlation with 1, 2, 39, 40 and 41.

A further selection of 36 peaks within the 41 peaks was performed based on a combination of loading plot in Fig. 3B and D. These 36 peaks showed a range of correlations with saccharification (Fig. 3D). Fig. 3D displays the PCA relationships between all peaks detected and saccharification. Unknown (6), furfural (8), 2-furanmethanol (9) and 1,2

cyclopentanedione (11) (mostly C-derived compounds) grouped together in the top of right-hand side in Fig. 3 D, showing that they are positively correlated with themselves and with saccharification. While acetic acid, methyl ester (3), 3-furaldehyde (7), phenol (14), 2,6-dimethoxyphenol (24), 2-methoxy-4-(1-propenyl)-phenol (28), 1-(4-hydroxy-3-methoxyphenyl)-2-propanone (30), 3',5'-dimethoxyacetophenone (31) and (E)-2,6-dimethoxy-4-(prop-1-en-1-yl) phenol (34) (group 2, mostly L-derived compounds) are situated in the top of left-hand side are positively correlated with themselves, but inversely correlated with saccharification.

3.2.2. Combined analysis of saccharification, silica content, hydroxycinnamic acids and pyrolysis peaks

A series of biomass components are well known to determine biomass saccharification. Among them, silica and hydroxycinnamic acids are some of the best-known factors that determine digestibility. In order to integrate these biomass components into our Pyr based analysis, we determined the Si content by XRF, analyzed hydroxycinnamic acids in all the samples, and integrated them in our PCA. Si content in the PhilRice association panel ranges between 3.6 and 8.7 %, showing a variation of 2.4-fold (Supplementary Table S1). This indicates that silica content is genotype specific and could be selected as an independent trait. FA and CA content ranged between 0.78 and 3.99 mg/g and 2.85–8.95 mg/g respectively. Principal component analysis was performed to establish the relationships between biomass components and saccharification. Fig. 4 A and B, show the score and loading plots between Si content, FA, CA, and saccharification. Using a combination of both (correlation and loading plot) we found that Si, CA and FA, are positively correlated with one another and negatively correlated with saccharification.

In Fig. 3 B and D we showed that compounds in the C group (3, 8, 9, 11, 16, 18, 23) are positively correlated with themselves and with compounds in the L group (14, 19, 24, 26) (Fig. 3 B and D). A similar relationship between pyrolysis products was found in the PCA correlation loading in Fig. 4 D. Fig. 4C and D show the relationships between the subset of 36 pyrolysis derived compounds, Si, FA, CA and saccharification. The peaks that group together in the left quadrant (lower) have similar weight in the analysis and correlate. Compounds such as 3-methylcyclopentane-1,2-dione (16), 2-cyclopenten-1-one, 2-hydroxy-3,4-dimethyl (18), furfural (8), catechol (19), 3-hydroxy-4-methoxy-benzaldehyde (26) and 2,6-dimethoxyphenol (24) are positively correlated with Si, FA and CA and a significant negative correlation with saccharification (Fig. 4C). The same is true for peaks 1 and 2 in the left quadrant (upper) indicating that they are inversely related to saccharification but in a different manner to either of others picks, the hydroxycinnamic acids, or silica content (Table 3). Peaks are closer to the center of the plot indicating a weak correlation with saccharification.

4. Discussion

In the present work, we have used a novel approach to study cell wall components in a rice diversity panel by combining Pyr-GC/MS with high throughput saccharification, Si determination and hydroxycinnamic acid content. Pyr-GC/MS is a technique used in polymer analysis that was adapted to characterize large sets of lignocellulose samples [27–29]. In the present paper we used Pyr-GC/MS combined with PCA to analyse 645 samples (the rice association panel comprises 215 accessions) and explore the suitability of identify fingerprinting related with straw recalcitrance. Being this is the first time that this “phenomics” approach is used in rice straw.

The pyrolysis of rice straw involves the cleavage of carbohydrates and lignin in complex reactions through several pathways [41–43]. A total of 71 compounds were identified through GC-MS and classified into three classes according to the fraction from which they originated: Carbohydrate (C), Lignin (L) and Others (O) (Table 1). C and L compounds were the major classes present in all samples, contributing 38.03% and 25.35% respectively. O compounds were ca. 15.49% and U

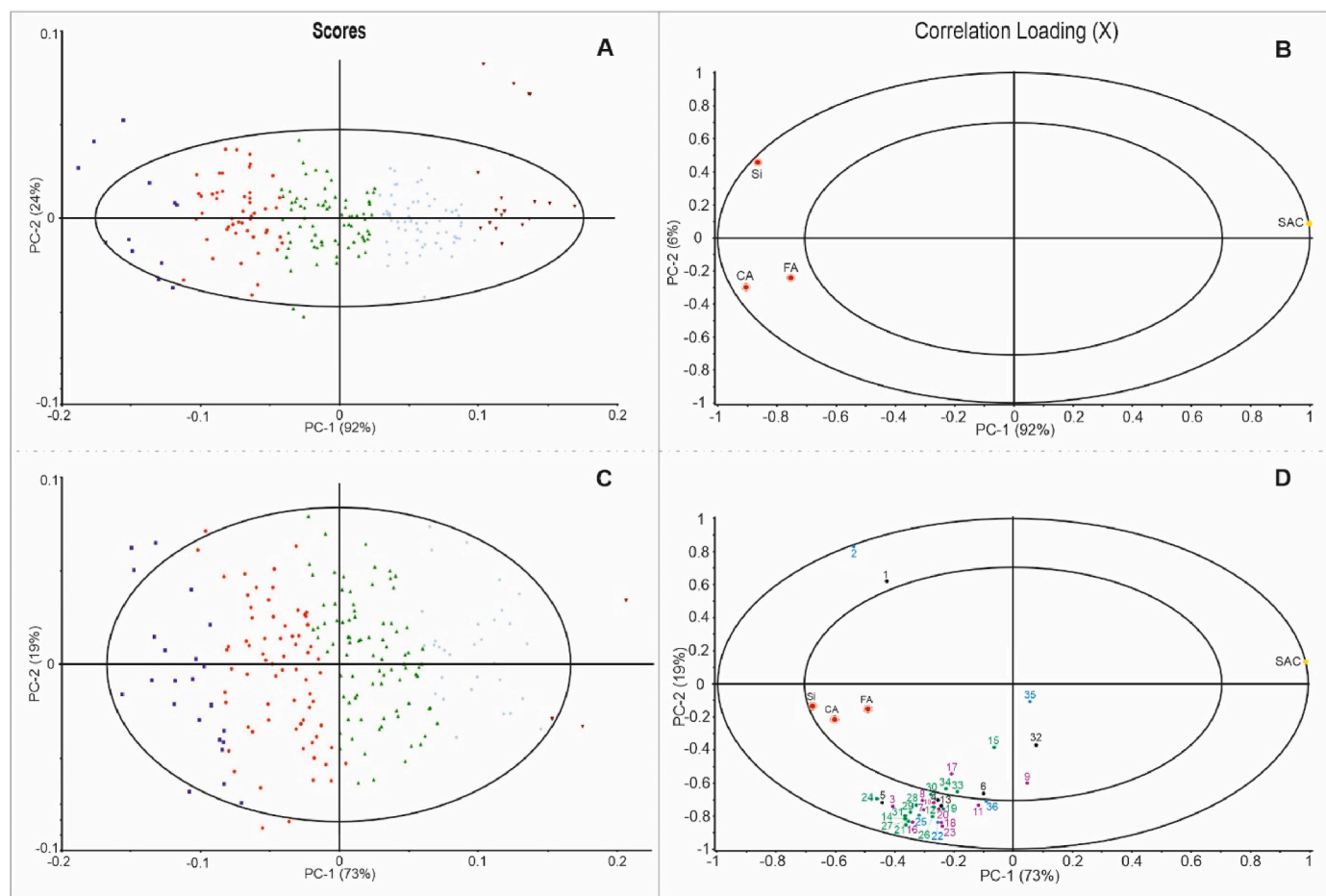


Fig. 4. Principal component regression analysis of Si, ferulic acid, p-coumaric acid, saccharification and a subset of 36 pyrolysis derived compounds. A–C: Score plots, the clusters of accessions are represented by dots of the same color and shape. B–D: Loading plots, peaks are labelled in different colours according to their origins: derived from Carbohydrate (purple), Lignin (green), Other (blue), and Unknown (black). Si, ferulic acid, p-coumaric acid (red) and saccharification (yellow). (For interpretation of the references to color in this figure legend, the reader is referred to the Web version of this article.)

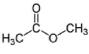
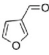
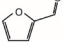
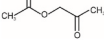
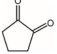
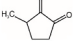
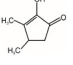
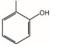
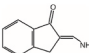

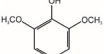
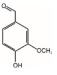
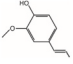
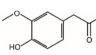
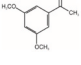
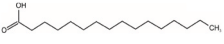
22.53%. The decomposition of lignin generated a mixture of syringol and guaiacol derivatives such as, catechol (19), 3-hydroxy-4-methoxybenzaldehyde (26) and 2,6-dimethoxyphenol (24). Derivatives of syringol and guaiacol have been found to form between 200 and 450 °C [43,44]. Syringol is typically detected at low temperatures (275–350 °C) [45,46] and the maximum rate of phenol formation occurs between 360 and 400 °C [47,48]. The importance of lignin composition in the determination of saccharification has been underlined by several publications in monocotyledonous species, in particular the non-alkaline extractable fraction of lignin [49,50]. The products of cellulose and hemicellulose pyrolysis identified in the C group included, 3-methyl-1,2-cyclopentanone (11), 2-hydroxy-3,4-dimethyl-2-cyclopentan-1-one (18), acetic acid, methyl ester (3), acetone and furfural (8). Within this C-derived group, anhydrosugars did not represent a significant fraction. This observation indicates that the formation of anhydrosugars can be inhibited by the interaction of hemicellulose and cellulose during pyrolysis, reducing their yields [48]. In parallel to phenotyping the PhilRice association panel using Pyr-GC/MS, we determined the saccharification potential using a HT automated approach [8]. The saccharification values found in the PhilRice panel are within the range found for rice in these previous studies [38]. To explore associations between pyrolysis products and saccharification we used principal component analysis (PCA). The combination of pyrolysis, PCA and saccharification allowed to identify 36 compounds as specific markers for carbohydrates and lignin derivatives (Fig. 3). C-derived compounds such as furfural (8), 2-furanmethanol (9) and 1,2-

cyclopentanone (11), were correlated directly with saccharification. While L-derived compounds such as phenol (14), 2,6-dimethoxyphenol (24), 2-methoxy-4-(1-propenyl)-phenol (28), 1-(4-hydroxy-3-methoxyphenyl)-2-propanone (30), 3',5'-dimethoxyacetophenone (31) and (E)-2,6-dimethoxy-4-(prop-1-en-1-yl) phenol (34) showed an inverse correlation with saccharification, acknowledging that saccharification could be restricted by L-derived compounds.

Since FA, CA and Si are the most studied components of biomass in relation to recalcitrance and digestibility properties to biomass [51], we evaluated the correlations of the content of FA, CA and Si with saccharification and the 36 compounds by PCA. Our correlation analysis shows that saccharification is significantly restricted by FA, CA and Si across the association panel (Fig. 4A–B). Hydroxycinnamic acids can be covalently linked to different components of the cell wall, and the carboxyl group at the end of its propenyl group provides the ability to esterify hemicellulose and lignin [52]. FA strengthens the plant cell wall by crosslinking arabinoxylans and lignin [53]. CA, in turn, has been proposed to facilitate lignin polymerisation by acting as a radical catalyst [54]. On the other hand, Si is a physical barrier to saccharification that is mostly located in the cuticle on the rice straw and protects the inner tissues of the straw [55]. In our work, Si represents a large proportion of rice straw and in our association panel it ranges between 3.6 and 8.7%. The relationships between the subset of 36 pyrolysis derived compounds, Si, FA, CA and saccharification (Fig. 4C–D) allowed to identify 16 compounds as fingerprints for recalcitrance and digestibility properties in the rice straw investigated (Table 3). Compounds such as

Table 3

Peak list of subsets of 28 compounds from PCA of saccharification, silica content, hydroxycinnamic acids and pyrolysis peaks. Number PCA (NP), compound names (NIST 14 library database -Match $\geq 85\%$ -), peaks are derived from Carbohydrate (C), Lignin (L) and Other (O).

NP	Name	From	Structure	Correlated	
				Si, FA CA	SAC
1	Unknown	U		+	-
2	oxygenated compounds	O		+	-
3	acetic acid, methyl ester	C		+	-
4	Unknown	U		+	-
5	Unknown	U		+	-
7	3-furaldehyde	C		+	-
8	furfural	C		+	-
10	1- acetyloxy, 2-propanone	C		+	-
11	1,2 cyclopentanedione	C		+	-
12	aromatic hydrocarbons	L		+	-
13	Unknown	U		+	-
16	3-methylcyclopentane-1,2-dione	C		+	-
18	2-cyclopenten-1-one, 2-hydroxy-3,4-dimethyl	C		+	-
19	catechol	L		+	-
20	oxygenated compound	C		+	-
21	aromatic hydrocarbons	L		+	-
22	2,3-dihydro, 1H-inden-1-one	O		+	-
23	furans	C		+	-
24	2,6-dimethoxy, phenol	L		+	-
25	oxygenated compound	O		+	-
26	3-hydroxy-4-methoxy-benzaldehyde	L		+	-
27	hydrocarbons derivative	L		+	-
28	2-methoxy-4-(1-propenyl)-phenol	L		+	-
29	aromatic hydrocarbons	L		+	-
30	1-(4-hydroxy-3-methoxyphenyl)-2-propanone	L		+	-
31	3',5'-dimethoxyacetophenone	L		+	-
36	n-hexadecanoic acid	O		+	-

3-methylcyclopentane-1,2-dione (16), 2-cyclopenten-1-one, 2-hydroxy-3,4-dimethyl (18), furfural (8), catechol (19), 3-hydroxy-4-methoxy-benzaldehyde (26) and 2,6-dimethoxyphenol (24) positively correlated with Si, FA and CA and negatively correlated with saccharification (Fig. 4C) can be used as fingerprints for recalcitrance.

5. Conclusion

In the present work, we explored the chemical basis of biomass recalcitrance using a Philippine rice association panel, involving high throughput pyrolysis followed by GC/MS and multivariate data analysis. This novel approach to lignocellulose analysis allowed for the identification of metabolite fingerprinting of lignocellulose has the advantage of providing a fingerprint of the complex chemical nature of rice straw.

This study highlights the insights generated by using PCA on Pyr-GC/MS data to correlate pyrolysis derived products with biomass composition. We have determined the correlation of biomass components such as Si and hydroxycinnamic acids with saccharification and pyrolysis products. The compositional variation in the population, reflected in the abundance of pyrolysis products derived from different fractions of the biomass, determines the saccharification potential.

Our results shed light not only on the biomass components that underpin the recalcitrance in rice straw, but also to the pyrolysis derivatives that are associated with this trend. This knowledge represents a toolkit for the selection of more digestible varieties, as well as a new trait that can assist in the speeding of breeding programs that target biomass valorization.

Availability of data and materials

All data generated or analyzed during this study are included in this published article and its Additional file 1.

Declarations

Ethics approval and consent to participate.
Not applicable.

Consent for publication

Not applicable.

CRedit authorship contribution statement

Mariana P. Silva: Conceptualization, Data curation, Formal analysis, Investigation, Methodology, Writing – original draft. **Caragh Whitehead:** Formal analysis, Investigation, Methodology, Writing – review & editing. **Reynante L. Ordonio:** Conceptualization, Data curation, Investigation, Methodology, Resources, Writing – review & editing. **Trinidad C. Fernando:** Investigation, Resources. **Mark Philip B. Castillo:** Investigation, Resources. **Jeremias L. Ordonio:** Formal analysis, Investigation, Resources. **Tony Larson:** Data curation, Validation, Writing – review & editing. **Daniel J. Upton:** Formal analysis, Investigation, Writing – review & editing. **Susan E. Hartley:** Conceptualization, Formal analysis, Supervision, Writing – review & editing. **Leonardo D. Gomez:** Conceptualization, Formal analysis, Funding acquisition, Investigation, Methodology, Project administration, Resources, Supervision, Writing – original draft.

Declaration of competing interest

The authors declare that they have no competing interests.

Data availability

Data will be made available on request.

Acknowledgements

This research was supported by funding from the BBSRC through grants BB/P022499/1 and BB/N013689/1. LC-MS/MS analysis of hydroxycinnamic acids was enabled by the Centre of Excellence in Mass Spectrometry, created thanks to a major capital investment through Science City York, supported by Yorkshire Forward with funds from the Northern Way Initiative, and subsequent support from the Engineering and Physical Sciences Research Council (EP/K039660/1; EP/M028127/1). The authors are grateful to Raymond Sloan from the Biorenewables Development Center for his help with the Pyrolysis GC/MS analysis, Swen Langer for implementing the LCMSMS method for CA and FA, and Lorenz Gerber (Genome Institute of Singapore) for his help with the HT

GC/MS analysis. We are also grateful to the Plant Breeding and Biotechnology Division of Phil Rice for sharing their rice lines. Also, to Jonalyn C. Yabes (Phil Rice) for her help in processing and sending the initial batch of DNA samples, and to Dr. Manuel Jose C. Regalado (PhilRice) for facilitating this collaborative research.

Abbreviations

Pyr-GC/MS	analytical pyrolysis-Gas chromatography-mass spectrometry
PCA	principal component analysis
C	Carbohydrate
L	Lignin
O	Others
GHs	glycosyl hydrolases
2,6-DO	2,6-Dimethoxyphenol
COBL	cobra-like gene
GPI	encode glycosylphosphatidylinositol
A	acetone
SAC	saccharification potential
Si	silica
FA	ferulic acid
CA	p-coumaric acid

Appendix A. Supplementary data

Supplementary data to this article can be found online at <https://doi.org/10.1016/j.biombioe.2024.107099>.

References

- [1] G. Cao, X. Zhang, S. Gong, F. Zheng, Investigation on emission factors of particulate matter and gaseous pollutants from crop residue burning, *J. Environ. Sci.* 20 (1) (2008) 50–55.
- [2] B. Gadde, S. Bonnet, C. Menke, S. Garivait, Air pollutant emissions from rice straw open field burning in India, Thailand and the Philippines, *Environ. Pollut.* 157 (5) (2009) 1554–1558.
- [3] S. Yin, X. Wang, X. Zhang, M. Guo, M. Miura, Y. Xiao, Influence of biomass burning on local air pollution in mainland Southeast Asia from 2001 to 2016, *Environ. Pollut.* 254 (2019) 112949.
- [4] C.S. Bueno, T. Lafarge, Higher crop performance of rice hybrids than of elite inbreds in the tropics: 1. Hybrids accumulate more biomass during each phenological phase, *Field Crops Res.* 112 (2) (2009) 229–237.
- [5] A. Bhardwaj, T. Alam, V. Sharma, M.S. Alam, H. Hamid, G.K. Deshwal, Lignocellulosic agricultural biomass as a biodegradable and eco-friendly alternative for polymer-based food packaging, *Journal of Packaging Technology and Research* 4 (2) (2020) 205–216.
- [6] J.F. Ma, N. Yamaji, K. Tamai, N. Mitani, Genotypic difference in silicon uptake and expression of silicon transporter genes in rice, *Plant Physiol.* 145 (3) (2007) 919–924.
- [7] L.D. Gomez, C.G. Steele-King, S.J. McQueen-Mason, Sustainable liquid biofuels from the writing's on the walls, *New Phytol.* 178 (3) (2008) 473–485.
- [8] L.D. Gomez, C. Whitehead, A. Barakate, C. Halpin, S.J. McQueen-Mason, Automated saccharification assay for determination of digestibility in plant materials, *Biotechnol. Biofuels* 3 (1) (2010) 23.
- [9] P.J. Smith, H.-T. Wang, W.S. York, M.J. Peña, B.R. Urbanowicz, Designer biomass for next-generation biorefineries: leveraging recent insights into xylan structure and biosynthesis, *Biotechnol. Biofuels* 10 (1) (2017) 286.
- [10] R.R. Schendel, M.R. Meyer, M. Bunzel, Quantitative profiling of feruloylated arabinoxylan side-chains from graminaceous cell walls, *Front. Plant Sci.* 6 (1249) (2016).
- [11] J. Ralph, Hydroxycinnamates in lignification, *Phytochemistry Rev.* 9 (2009) 65–83.
- [12] R. Zhang, H. Gao, Y. Wang, B. He, J. Lu, W. Zhu, L. Peng, Y. Wang, Challenges and perspectives of green-like lignocellulose pretreatments selectable for low-cost biofuels and high-value bioproduction, *Bioresour. Technol.* 369 (2023) 128315.
- [13] M.E. Vega-Sánchez, P.C. Ronald, Genetic and biotechnological approaches for biofuel crop improvement, *Curr. Opin. Biotechnol.* 21 (2) (2010) 218–224.
- [14] P. Daly, C. McClellan, M. Maluk, H. Oakey, C. Lapiere, R. Waugh, J. Stephens, D. Marshall, A. Barakate, Y. Tsuji, G. Goeminne, R. Vanholme, W. Boerjan, J. Ralph, C. Halpin, RNAi-suppression of barley caffeic acid O-methyltransferase modifies lignin despite redundancy in the gene family, *Plant Biotechnol. J.* 17 (3) (2019) 594–607.
- [15] R. Bhatia, J.A. Gallagher, L.D. Gomez, M. Bosch, Genetic engineering of grass cell wall polysaccharides for biorefining, *Plant Biotechnol. J.* 15 (9) (2017) 1071–1092.
- [16] Y. Wang, P. Liu, G. Zhang, Q. Yang, J. Lu, T. Xia, L. Peng, Y. Wang, Cascading of engineered bioenergy plants and fungi sustainable for low-cost bioethanol and

- high-value biomaterials under green-like biomass processing, *Renew. Sustain. Energy Rev.* 137 (2021) 110586.
- [17] F.P. Massey, S.E. Hartley, Experimental demonstration of the antiherbivore effects of silica in grasses: impacts on foliage digestibility and vole growth rates, *Proc. Biol. Sci.* 273 (1599) (2006) 2299–2304.
- [18] J. Zhang, W. Zou, Y. Li, Y. Feng, H. Zhang, Z. Wu, Y. Tu, Y. Wang, X. Cai, L. Peng, Silica distinctively affects cell wall features and lignocellulosic saccharification with large enhancement on biomass production in rice, *Plant Sci.* 239 (2015) 84–91.
- [19] Zahoor, D. Sun, Y. L., J. Wang, Y. Tu, Y. Wang, Z. Hu, S. Zhou, L. Wang, G. Xie, J. Huang, A. Alam, L. Peng, Biomass saccharification is largely enhanced by altering wall polymer features and reducing silicon accumulation in rice cultivars harvested from nitrogen fertilizer supply, *Bioresour. Technol.* 243 (2017) 957–965.
- [20] B.R. Moreira, M.C. Breitzkreitz, R. Simister, S.J. McQueen-Mason, L.D. Gomez, C. A. Rezende, Improved hydrolysis yields and silica recovery by design of experiments applied to acid-alkali pretreatment in rice husks, *Ind. Crop. Prod.* 170 (2021) 113676.
- [21] S. Reidinger, M.H. Ramsey, S.E. Hartley, Rapid and accurate analyses of silicon and phosphorus in plants using a portable X-ray fluorescence spectrometer, *New Phytol.* 195 (3) (2012) 699–706.
- [22] A. López-Malvar, R. Santiago, R.A. Malvar, D. Martín, I. Pereira dos Santos, L. A. Batista de Carvalho, L. Faas, L.D. Gómez, R.M. da Costa, FTIR screening to elucidate compositional differences in maize recombinant inbred lines with contrasting saccharification efficiency yields, *Agronomy* 11 (6) (2021) 1130.
- [23] J. Huang, T. Xia, A. Li, B. Yu, Q. Li, Y. Tu, W. Zhang, Z. Yi, L. Peng, A rapid and consistent near infrared spectroscopic assay for biomass enzymatic digestibility upon various physical and chemical pretreatments in *Miscanthus*, *Bioresour. Technol.* 121 (2012) 274–281.
- [24] Z. Hu, Y. Wang, J. Liu, Y. Li, Y. Wang, J. Huang, Y. Ai, P. Chen, Y. He, M.N. Aftab, Integrated NIRS and QTL assays reveal minor mannose and galactose as contrast lignocellulose factors for biomass enzymatic saccharification in rice, *Biotechnol. Biofuels* 14 (1) (2021) 144.
- [25] J. Huang, Y. Li, Y. Wang, Y. Chen, M. Liu, Y. Wang, R. Zhang, S. Zhou, J. Li, Y. Tu, A precise and consistent assay for major wall polymer features that distinctively determine biomass saccharification in transgenic rice by near-infrared spectroscopy, *Biotechnol. Biofuels* 10 (1) (2017) 1–14.
- [26] W. Chen, Y. Gao, W. Xie, L. Gong, K. Lu, W. Wang, Y. Li, X. Liu, H. Zhang, H. Dong, W. Zhang, L. Zhang, S. Yu, G. Wang, X. Lian, J. Luo, Genome-wide association analyses provide genetic and biochemical insights into natural variation in rice metabolism, *Nat. Genet.* 46 (7) (2014) 714–721.
- [27] L. Gerber, M. Eliasson, J. Trygg, T. Moritz, B. Sundberg, Multivariate curve resolution provides a high-throughput data processing pipeline for pyrolysis-gas chromatography/mass spectrometry, *J. Anal. Appl. Pyrol.* 95 (2012) 95–100.
- [28] L. Gerber, D. Öhman, M. Kumar, P. Ranocha, D. Goffner, B. Sundberg, High-throughput microanalysis of large lignocellulosic sample sets by pyrolysis-gas chromatography/mass spectrometry, *Physiol. Plantarum* 156 (2) (2016) 127–138.
- [29] R.C. Pinto, L. Gerber, M. Eliasson, B. Sundberg, J. Trygg, Strategy for minimizing between-study variation of large-scale phenotypic experiments using multivariate analysis, *Anal. Chem.* 84 (20) (2012) 8675–8681.
- [30] S. Fry, *The Growing Plant Cell Wall: Chemical and Metabolic Analysis*, Longman, London, 2000.
- [31] L.D. Gomez, C. Whitehead, A. Barakate, C. Halpin, S.J. McQueen-Mason, Automated saccharification assay for determination of digestibility in plant materials, *Biotechnol. Biofuels* 3 (2010) 23.
- [32] M.P. Silva, M.L.N. Lobos, T.R. Larson, S. McQueen-Mason, L.D. Gomez, E. L. Moyano, A.L. Scopel, Valuable chemicals identified from *Flourensia* species using vacuum and analytical pyrolysis, *J. Anal. Appl. Pyrol.* 161 (2022) 105382.
- [33] M.C. Chambers, B. Maclean, R. Burke, D. Amodei, D.L. Ruderman, S. Neumann, L. Gatto, B. Fischer, B. Pratt, J. Egerton, K. Hoff, D. Kessner, N. Tasman, N. Shulman, B. Frewen, T.A. Baker, M.Y. Brusniak, C. Paulse, D. Creasy, L. Flashner, K. Kani, C. Moulding, S.L. Seymour, L.M. Nuwaysir, B. Lefebvre, F. Kuhlmann, J. Roark, P. Rainer, S. Detlev, T. Hemenway, A. Huhmer, J. Langridge, B. Connolly, T. Chadick, K. Holly, J. Eckels, E.W. Deutsch, R. L. Moritz, J.E. Katz, D.B. Agus, M. MacCoss, D.L. Tabb, P. Mallick, A cross-platform toolkit for mass spectrometry and proteomics, *Nat. Biotechnol.* 30 (10) (2012) 918–920.
- [34] C.A. Smith, E.J. Want, G. O'Maille, R. Abagyan, G. Siuzdak, XCMS: processing mass spectrometry data for metabolite profiling using nonlinear peak alignment, matching, and identification, *Anal. Chem.* 78 (3) (2006) 779–787.
- [35] R. Tautenhahn, C. Böttcher, S. Neumann, Highly sensitive feature detection for high resolution LC/MS, *BMC Bioinf.* 9 (1) (2008) 504.
- [36] C. Kuhl, R. Tautenhahn, C. Böttcher, T.R. Larson, S. Neumann, CAMERA: an integrated strategy for compound spectra extraction and annotation of liquid chromatography/mass spectrometry data sets, *Anal. Chem.* 84 (1) (2012) 283–289.
- [37] R.S. Fukushima, R.D. Hatfield, Comparison of the acetyl bromide spectrophotometric method with other analytical lignin methods for determining lignin concentration in forage samples, *J. Agric. Food Chem.* 52 (12) (2004) 3713–3720.
- [38] D.T. Nguyen, L.D. Gomez, A. Harper, C. Halpin, R. Waugh, R. Simister, C. Whitehead, H. Oakey, H.T. Nguyen, T.V. Nguyen, T.X. Duong, S.J. McQueen-Mason, Association mapping identifies quantitative trait loci (QTL) for digestibility in rice straw, *Biotechnol. Biofuels* 13 (1) (2020) 165.
- [39] M. Ghalibaf, T.R.K.C. Doddapaneni, R. Alén, Pyrolytic behavior of lignocellulosic-based polysaccharides, *J. Therm. Anal. Calorim.* 137 (1) (2019) 121–131.
- [40] S. Tianniam, T. Bamba, E. Fukusaki, Pyrolysis GC-MS-based metabolite fingerprinting for quality evaluation of commercial *Angelica acutiloba* roots, *J. Biosci. Bioeng.* 109 (1) (2010) 89–93.
- [41] M. Brebu, C. Vasile, Thermal degradation of lignin – a Review, *Cellul. Chem. Technol.* 44 (2010) 353–363.
- [42] Q. Lu, X.-c. Yang, C.-q. Dong, Z.-f. Zhang, X.-m. Zhang, X.-f. Zhu, Influence of pyrolysis temperature and time on the cellulose fast pyrolysis products: analytical Py-GC/MS study, *Journal of Analytical and Applied Pyrolysis - J ANAL APPL PYROL* 92 (2011) 430–438.
- [43] A. Lourenço, J. Gominho, H. Pereira, Chemical Characterization of Lignocellulosic Materials by Analytical Pyrolysis, 2018.
- [44] H. Kawamoto, Lignin pyrolysis reactions, *J. Wood Sci.* 63 (2) (2017) 117–132.
- [45] M. Carrier, M. Windt, B. Ziegler, J. Appelt, B. Saake, D. Meier, A. Bridgwater, Quantitative insights into the fast pyrolysis of extracted cellulose, Hemicelluloses, and Lignin, *ChemSusChem* 10 (16) (2017) 3212–3224.
- [46] D. Mohan, C.U. Pittman Jr., P.H. Steele, Pyrolysis of wood/biomass for bio-oil: a critical review, *Energy Fuels* 20 (3) (2006) 848–889.
- [47] D.K. Shen, S. Gu, K.H. Luo, S.R. Wang, M.X. Fang, The pyrolytic degradation of wood-derived lignin from pulping process, *Bioresour. Technol.* 101 (15) (2010) 6136–6146.
- [48] F.-X. Collard, J. Blin, A review on pyrolysis of biomass constituents: mechanisms and composition of the products obtained from the conversion of cellulose, hemicelluloses and lignin, *Renew. Sustain. Energy Rev.* 38 (2014) 594–608.
- [49] Z. Li, C. Zhao, Y. Zha, C. Wan, S. Si, F. Liu, R. Zhang, F. Li, B. Yu, Z. Yi, The minor wall-networks between monolignols and interlinked-phenolics predominantly affect biomass enzymatic digestibility in *Miscanthus*, *PLoS One* 9 (8) (2014) e105115.
- [50] J. Jia, B. Yu, L. Wu, H. Wang, Z. Wu, M. Li, P. Huang, S. Feng, P. Chen, Y. Zheng, Biomass enzymatic saccharification is determined by the non-KOH-extractable wall polymer features that predominately affect cellulose crystallinity in corn, *PLoS One* 9 (9) (2014) e108449.
- [51] L.E. Bartley, M.L. Peck, S.R. Kim, B. Ebert, C. Manisseri, D.M. Chiniy, R. Sykes, L. Gao, C. Rautengarten, M.E. Vega-Sánchez, P.I. Benke, P.E. Canlas, P. Cao, S. Brewer, F. Lin, W.L. Smith, X. Zhang, J.D. Keasling, R.E. Jentoff, S.B. Foster, J. Zhou, A. Ziebell, G. An, H.V. Scheller, P.C. Ronald, Overexpression of a BAHD acyltransferase, *OsAt10*, alters rice cell wall hydroxycinnamic acid content and saccharification, *Plant Physiol.* 161 (4) (2013) 1615–1633.
- [52] D.M. de Oliveira, A. Finger-Teixeira, T. Rodrigues Mota, V.H. Salvador, F. C. Moreira-Vilar, H.B. Correa Molinari, R.A. Craig Mitchell, R. Marchiosi, O. Ferrarese-Filho, W. Dantas dos Santos, Ferulic acid: a key component in grass lignocellulose recalcitrance to hydrolysis, *Plant Biotechnol. J.* 13 (9) (2015) 1224–1232.
- [53] E. Allerding, J. Ralph, P.F. Schatz, D. Gniewchwitz, H. Steinhart, M. Bunzel, Isolation and structural identification of diabinosyl 8-O-4-dehydrodiferulate from maize bran insoluble fibre, *Phytochemistry* 66 (1) (2005) 113–124.
- [54] J. Ralph, Hydroxycinnamates in lignification, *Phytochemistry Rev.* 9 (1) (2010) 65–83.
- [55] P. Binod, R. Sindhu, R.R. Singhanian, S. Vikram, L. Devi, S. Nagalakshmi, N. Kurien, R.K. Sukumaran, A. Pandey, Bioethanol production from rice straw: an overview, *Bioresour. Technol.* 101 (13) (2010) 4767–4774.